

---

# Variance Reduction with Array-RQMC for Tau-Leaping Simulation of Stochastic Biological and Chemical Reaction Networks

Florian Puchhammer · Amal Ben Abdellah · Pierre L'Ecuyer

November 23, 2021

**Abstract** We explore the use of Array-RQMC, a randomized quasi-Monte Carlo method designed for the simulation of Markov chains, to reduce the variance when simulating stochastic biological or chemical reaction networks with  $\tau$ -leaping. We find that when the method is properly applied, variance reductions by factors in the thousands can be obtained. These factors are much larger than those observed previously by other authors who tried RQMC methods for the same examples. Array-RQMC simulates an array of realizations of the Markov chain and requires a sorting function to reorder these chains according to their states, after each step. The choice of a good sorting function is a key ingredient for the efficiency of the method. We illustrate this by comparing various choices. The expected number of reactions of each type per step also has an impact on the efficiency gain.

**Keywords** Chemical reaction networks · stochastic biological systems · variance reduction · Quasi-Monte Carlo · Array-RQMC · Tau-leaping · continuous-time Markov chains · Gillespie

## 1 Introduction

We consider systems of chemical species whose molecule numbers dynamically change over time as the molecules react via a set of predefined chemical equations. The evolution of such systems is typically modeled by a *continuous-time Markov chain* (CTMC) (Gillespie, 1977; Anderson, 1991; Anderson and Kurtz, 2011) whose state is a vector that gives the number

---

F. Puchhammer,  
Basque Center for Applied Mathematics, Alameda de Mazarredo 14, 48009 Bilbao, Basque Country, Spain;  
and DIRO, Université de Montréal, C.P. 6128, Succ. Centre-Ville, Montréal, H3C 3J7, Canada  
E-mail: fpuchhammer@bcmath.org

A. Ben Abdellah  
DIRO, Université de Montréal, C.P. 6128, Succ. Centre-Ville, Montréal, H3C 3J7, Canada  
E-mail: amal.ben.abdellah@umontreal.ca

P. L'Ecuyer  
DIRO, Université de Montréal, C.P. 6128, Succ. Centre-Ville, Montréal, H3C 3J7, Canada  
E-mail: lecuyer@iro.umontreal.ca

of copies of each species. Each transition (or jump) of the CTMC corresponds to the occurrence of one reaction, and the occurrence rate of each potential reaction (also called the *reaction propensity*) is a function of the state of the chain. The probability that any given reaction is the next one that will occur is proportional to its propensity and the time until the next reaction has an exponential distribution whose rate is the sum of these propensities. The *stochastic simulation algorithm* (SSA) of Gillespie (1977) simulates the successive transitions of this CTMC one by one, by generating the exponential time until the next reaction and determining independently which reaction it is. This method is exact (there is no bias). But when the number of molecules is large, simulating all the reactions one by one is often too slow, because their frequency is too high. One popular alternative is to approximate the CTMC by a *discrete-time Markov chain* (DTMC), as follows. Fix a time interval  $\tau > 0$ . Under the simplifying assumption that the rates of the different reactions do not change during the next  $\tau$  units of time, the numbers of occurrences for each type of reaction are independent Poisson random variables with means that are  $\tau$  times the occurrence rates (or propensities) of these reactions. Each step (or transition) of the DTMC corresponds to  $\tau$  units of time for the CTMC. This DTMC can be simulated by generating a vector of independent Poisson random variables at each step, and updating the state to reflect all the reactions that occurred during this time interval. In the setting of chemical reaction networks, this approach is the  *$\tau$ -leaping method* of Gillespie (2001), and it is widely used in practice. This is the method we consider in this paper.

There are several other approximation methods, some of them leading to simpler and faster simulations, but the error and/or bias can also be more significant (Gillespie, 2000; Higham, 2008). One simple approach uses a fluid approximation in which the copy numbers are assumed to take real values that vary in time according to a system of deterministic differential equations called the *reaction rate equations* which can be simulated numerically (Gillespie, 2000; Higham, 2008). This type of deterministic model is the primary tool in the field of system dynamics, and it is widely used in many areas. It corresponds to chemical kinetics equations found in textbooks. But this model ignores randomness, so it cannot capture the stochastic variations observed in experiments with real systems (Beentjes and Baker, 2019). Noise can be introduced via a *stochastic differential equations* model, which amounts essentially to approximate the Poisson distribution by a normal one, and the denumerable-state CTMC by a continuous-state process. This leads to the *chemical Langevin equation* (Gillespie, 2000; Beentjes and Baker, 2019), which can be simulated efficiently by standard methods for stochastic differential equations (Kloeden and Platen, 1992) and may provide a reasonable approximation when the number of molecules of each type is very large, but can otherwise suffer from bias.

The purpose of the stochastic simulations with  $\tau$ -leaping could be for example to estimate the probability distribution of the state at a given time  $t$ , or the probability that the state is in a given subset at time  $t$ , or perhaps the expectation of some function of the state. The simulations are usually done via Monte Carlo (MC) sampling, using a random number generator that provides a good imitation of independent uniform random variables over the interval  $(0, 1)$  (L'Ecuyer, 2012). For MC estimators based on the average over  $n$  independent samples, the variance and the standard deviation converge as  $\mathcal{O}(n^{-1})$  and  $\mathcal{O}(n^{-1/2})$ , respectively, which is rather slow.

*Randomized quasi-Monte Carlo* (RQMC) provides an alternative sampling approach which under favorable conditions can improve this convergence rate of the variance to  $\mathcal{O}(n^{-2+\varepsilon})$  for any  $\varepsilon > 0$ , and even better in special situations (Owen, 1997, 2003; L'Ecuyer and Lemieux, 2002; L'Ecuyer, 2009, 2018). *Quasi-Monte Carlo* (QMC) replaces the  $n$  independent vectors of uniform random numbers that drive the simulations by  $n$  *deterministic* vectors with

a sufficient number of coordinates to simulate the system and which cover the space (the unit hypercube) more evenly than typical independent random points (Niederreiter, 1992; Dick and Pillichshammer, 2010). RQMC randomizes these points in a way that each individual point becomes a vector of independent uniform random numbers, while at the same time the set of points as a whole retains its structure and high uniformity. As a result, RQMC can provide an unbiased estimator with lower variance.

On the other hand, there are two important limitations. Firstly, the  $\mathcal{O}(n^{-2+\varepsilon})$  convergence rates for RQMC are proved only under conditions that the integrand is a smooth function of the uniforms, whereas when simulating the CTMC considered here, the sequence of states that are visited is discontinuous in the underlying uniform random variates. Secondly, when the points are high-dimensional and some high-order interactions between the coordinates are important, the variance reduction is usually limited, and this often happens when simulating the CTMCs that model reaction networks via either direct SSA or  $\tau$ -leaping. Indeed, those simulations require at least one or two random numbers per step of the chain, the number of steps can be very large in real applications, so the dimension of the points, which is the total number of random numbers that are required to simulate one realization of the process, can be very large. Beentjes and Baker (2019) investigated the performance of  $\tau$ -leaping combined with traditional RQMC and found that the gain from RQMC compared to MC was small. They mentioned the two limitations above as possible explanations for this behavior.

The *Array-RQMC* algorithm (L'Ecuyer et al, 2006, 2008, 2009) has been developed precisely to recapture the power of RQMC when simulating Markov chains over a large number of steps, as in the problem considered here. The empirical variance under Array-RQMC has been observed to converge faster than under MC in several examples from various areas, sometimes at the  $n^{-2+\varepsilon}$  rate, even for some examples where the cost function was discontinuous (Demers et al, 2005; L'Ecuyer et al, 2007, 2008, 2009; Dion and L'Ecuyer, 2010; L'Ecuyer et al, 2018; Ben Abdellah et al, 2019). The faster convergence has also been proven theoretically under certain conditions (L'Ecuyer et al, 2008).

Our present work was motivated by Beentjes and Baker (2019) and our aim is to see how Array-RQMC can improve upon MC and classical RQMC, first by using the same examples as in their paper. Hellander (2008) also experimented with Array-RQMC, in combination with uniformization of the CTMC and conditional Monte Carlo (CMC) based on the discrete-time conversion method of Fox and Glynn (1990). Their goal was to estimate the probability distribution of the state at a fixed time  $t > 0$ . In this setting, CMC alone provably reduces the variance. Empirically, with CMC, they obtained variance reductions by factors of about 20 in one example and 45 in another example. With the combination of CMC with Array-RQMC, they observed variance reductions by a factor of about 100 with  $n = 10^5$  for both examples. Thus, Array-RQMC provides an additional gain on top of CMC, by a factor of about 2.5 to 5.

In this paper, we show how to obtain much larger variance-reduction factors with Array-RQMC. We do this in the same setting as Beentjes and Baker (2019), where the  $\tau$ -leaping method is used to estimate an expectation at a given time  $t$ . We find empirically that the combination of  $\tau$ -leaping with the Array-RQMC algorithm can bring not only a significant variance reduction, but also an improved convergence rate, compared with plain MC.

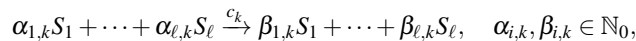
The main idea of the Array-RQMC algorithm is to simulate  $n$  copies of the Markov chain in parallel, in a way that the empirical distribution of the chain's states at any given step is closer to the exact theoretical distribution at that step than with ordinary MC. To achieve this, at each step, the first few coordinates of the RQMC point set are designated to match the points to the states, and the remaining coordinates are used to advance the

chains by one step. This matching can be interpreted as sorting the chains in some particular order, to match the ordering of the RQMC points. In the simple case where the state is one-dimensional, it suffices to enumerate the points by increasing order of their first coordinate and sort the chains by increasing order of their state. For higher-dimensional states, one possibility is to use some kind of multivariate sort to order both the points and the states; we will describe some of these sorts in Section 3.2. Another approach is to define an *importance function*, which maps the state to a one-dimensional representative value, and sort the chains by that value. The choice of mapping can have a significant impact on the performance. If the mapping is fast to evaluate, this approach can reduce the computing time significantly, because a one-dimensional sort is usually much faster to execute than a multivariate one. To preserve the power of Array-RQMC, on the other hand, the importance function must provide a good estimate (or forecast) of the expected future value or cost, given the state at which it is evaluated. For this, it must be tailored to the problem at hand. A good tradeoff between simplicity and prediction accuracy is not always easy to achieve, but it is a key ingredient for the performance of Array-RQMC. As a proof of concept that this approach can work for reaction networks, we experiment with a very simple one-step look-ahead importance function, and we find that it works very well in all our examples. Empirically, in our experiments, this approach is often competitive with the best multivariate sorts in terms of variance reduction, and the sorting times are shorter, so it often provides the best efficiency improvement. We also discuss how more elaborate importance functions could be defined.

The remainder is structured as follows. In Section 2 we recall the fixed-step  $\tau$ -leaping method for the simulation of well-mixed reaction networks in its simplest form. In Section 3, we define the Array-RQMC method and discuss some of the most prominent multivariate sorting algorithms. In Section 4, we describe the methodology used for our experiments and provide numerical results, with a discussion. A conclusion follows.

## 2 The CTMC Model and the $\tau$ -Leaping Algorithm for Reaction Networks

We consider a system comprised of  $\ell \geq 1$  types of chemical species  $S_1, \dots, S_\ell$  that can react via  $d \geq 1$  reaction types (or channels)  $R_1, \dots, R_d$ . We assume that the species are well-mixed within a volume that does not change over time and whose temperature remains constant. Each reaction  $R_k$ ,  $k = 1, \dots, d$ , can be written as



where  $c_k > 0$  is the reaction rate constant for  $R_k$ . Let  $\mathbf{X}(t) = (X_1(t), \dots, X_\ell(t)) \in \mathbb{N}_0^\ell$ , where  $X_i(t)$  is the copy number (i.e., the number of molecules) of type  $S_i$  at time  $t$ , for  $i = 1, \dots, \ell$  and  $0 \leq t \leq T$ . The process  $\{\mathbf{X}(t), t \geq 0\}$  is modeled as a CTMC with fixed initial state  $\mathbf{X}(0) = \mathbf{x}_0$  and for which each jump corresponds to the occurrence of one reaction. The jump rate (or *propensity function*) for reaction  $R_k$  is a function  $a_k$  of the current state; it is  $a_k(\mathbf{x})$  when  $\mathbf{X}(t) = \mathbf{x}$ . This means that for a small  $\delta > 0$ , reaction  $R_k$  occurs exactly once during the time interval  $(t, t + \delta]$  with probability  $a_k(\mathbf{x})\delta + o(\delta)$  and occurs more than once with probability  $o(\delta)$ . When  $R_k$  occurs, the state changes from  $\mathbf{x}$  to  $\mathbf{x} + \zeta_k$ , where  $\zeta_k = (\beta_{1,k} - \alpha_{1,k}, \dots, \beta_{\ell,k} - \alpha_{\ell,k})$  is the stoichiometric vector for  $R_k$ . The standard for  $a_k(\mathbf{x})$ , which we assume in our examples, is  $a_k(\mathbf{x}) = c_k \langle_k(\mathbf{x})$  where  $\langle_k(\mathbf{x}) = \prod_{i=1}^{\ell} \binom{x_i}{\alpha_{i,k}}$  represents the number of ways of selecting the molecules for reaction  $R_k$  when in state  $\mathbf{x} = (x_1, \dots, x_\ell)$

(Higham, 2008). When in state  $\mathbf{x}$ , the time until the next reaction has an exponential distribution with rate  $\lambda(\mathbf{x}) = \sum_{k=1}^d a_k(\mathbf{x})$ , the probability that this reaction is  $R_k$  is  $a_k(\mathbf{x})/\lambda(\mathbf{x})$ , and these random variables are independent. The SSA of Gillespie (1977) simulates this CTMC directly. However, when a very large number of reactions occur in the time interval of interest, the direct simulation approach may be too slow.

Gillespie (2001) proposed the  $\tau$ -leaping algorithm as a way to speed up the simulation. This approach discretizes the time into intervals of length  $\tau > 0$ , and it generates directly the number of occurrences of each type of reaction in each such interval. If  $\mathbf{X}(t) = \mathbf{x}$  at the beginning of an interval, it is assumed (as an approximation) that the rate of each reaction  $R_k$  remains equal to  $a_k(\mathbf{x})$  during the entire interval  $[t, t + \tau]$ . Under this simplifying assumption, the number  $D_k$  of occurrences of  $R_k$  during this time interval has a Poisson distribution with mean  $a_k(\mathbf{x})\tau$ , and  $D_1, \dots, D_d$  are independent. These  $D_k$  can be simulated easily via the inversion method, by generating independent uniform random numbers over  $(0, 1)$  and applying the inverse of the cumulative distribution function (cdf) of the appropriate Poisson distribution (Giles, 2016). The simulated state at time  $t + \tau$  is then  $\mathbf{x} + \sum_{k=1}^d D_k \zeta_k$ . Repeating this at each step gives an approximating *discrete-time Markov chain* (DTMC)  $\{\mathbf{X}_j, j \geq 0\}$  defined by  $\mathbf{X}_0 = \mathbf{x}_0$  and

$$\mathbf{X}_j = \mathbf{X}_{j-1} + \sum_{k=1}^d D_{j,k} \zeta_k, = \mathbf{X}_{j-1} + \sum_{k=1}^d F_{j,k}^{-1}(U_{j,k}) \zeta_k \stackrel{\text{def}}{=} \varphi(\mathbf{X}_{j-1}, \mathbf{U}_j), \quad (1)$$

where  $D_{j,k} = F_{j,k}^{-1}(U_{j,k})$ ,  $F_{j,k}$  is the cdf of the Poisson distribution with mean  $a_k(\mathbf{X}_{j-1})\tau$ ,  $\mathbf{U}_j = (U_{j,1}, \dots, U_{j,d})$ , and the  $U_{j,k}$  are independent uniform random numbers over  $(0, 1)$ , for  $k = 1, \dots, d$  and  $j \geq 1$ . If  $\tau$  is small enough,  $\mathbf{X}_j$  has approximately the same distribution as  $\mathbf{X}(j\tau)$ , so this DTMC provides an approximate skeleton of a CTMC sample path.

This  $\tau$ -leaping approximation has some potential problems, because it introduces bias which can propagate across successive steps, and this bias can be important if  $\tau$  is not small enough. It is also possible to obtain negative copy numbers, i.e., some coordinates of some  $\mathbf{X}_j$  taking negative values. Adaptive strategies and modifications of the algorithm have been designed to prevent or handle this; see, e.g., (Anderson, 2008; Anderson and Higham, 2012; Beentjes and Baker, 2019), and the references given there. We do not discuss these techniques in this paper. Our main goal is to explore how Array-RQMC can be effectively combined with  $\tau$ -leaping, and we keep the setting simple to avoid distractions. In our experiments, we took  $\tau$  small enough so we did not observe negative copy numbers.

Following Beentjes and Baker (2019), we suppose that the objective is to estimate  $\mu = \mathbb{E}[g(\mathbf{X}(T))]$  for a given time  $T > 0$  and some function  $g: \mathbb{N}_0^\ell \rightarrow \mathbb{R}$ . These authors only took a coordinate projection for  $g$  (i.e., they only estimated expected copy numbers) in their examples, and we do the same, but what we do applies easily to other choices of  $g$ . For example,  $g(\mathbf{x})$  could be the indicator that  $\mathbf{x}$  belongs to a given set  $A$ , in which case  $\mu = \mathbb{P}[\mathbf{X}(T) \in A]$ . We take  $\tau = T/s$  where  $s$  is a positive integer that represents the number of steps of the DTMC that will be simulated. To estimate  $\mu$  with  $\tau$ -leaping and MC, we simulate  $n$  independent realizations of the DTMC via

$$\mathbf{X}_{i,0} = \mathbf{x}_0, \quad \mathbf{X}_{i,j} = \varphi_j(\mathbf{X}_{i,j-1}, \mathbf{U}_{i,j}) \quad \text{for } j = 1, \dots, s \text{ and } i = 0, \dots, n-1, \quad (2)$$

where the  $\mathbf{U}_{i,j}$ 's are independent uniform random points over  $(0, 1)^d$ . The estimator is

$$\hat{\mu}_n = \frac{1}{n} \sum_{i=0}^{n-1} g(\mathbf{X}_{i,s}). \quad (3)$$

We know that  $\mathbb{E}[\hat{\mu}_n] = \mathbb{E}[g(\mathbf{X}_s)] \approx \mathbb{E}[g(\mathbf{X}(T))] = \mu$  (we do not look at the bias  $\mathbb{E}[g(\mathbf{X}_s)] - \mathbb{E}[g(\mathbf{X}(T))]$  in this paper) and  $\text{Var}[\hat{\mu}_n] = \text{Var}[g(\mathbf{X}_s)]/n$ .

To use classical RQMC instead of MC, we simply replace the independent random points by a set of  $n$  vectors  $\mathbf{V}_i = (\mathbf{U}_{i,1}, \mathbf{U}_{i,2}, \dots, \mathbf{U}_{i,s})$ ,  $i = 1, \dots, n$ , which form an RQMC point set in  $sd$  dimensions, as did Beentjes and Baker (2019).

### 3 Array-RQMC to Simulate the DTMC

#### 3.1 The Array-RQMC Algorithm

We now explain how to apply Array-RQMC to simulate the DTMC via (2) and estimate  $\mathbb{E}[g(\mathbf{X}_s)] \approx \mu$  again with (3), but with a different sampling strategy for the random numbers. The algorithm simulates the  $n$  sample paths of the DTMC in parallel, using an  $(l+d)$ -dimensional RQMC point set to advance all the chains by one step at a time, for some  $l \in \{1, \dots, \ell\}$ . The first  $l$  coordinates of the points are used to make a one-to-one pairing between the chains and the points, and the other  $d$  coordinates are used to advance the chains. When  $l < \ell$ , one must first define a *dimension-reduction mapping*  $h: \mathbb{N}_0^\ell \rightarrow \mathbb{R}^l$  whose aim is to extract the most important features from the state and summarize them in a lower-dimensional vector which is used for the sort. For  $l = 1$ , the mapping  $h$  has been called an *importance function* or *sorting function* (L'Ecuyer et al, 2006, 2007, Section 3). At each step, both the RQMC points and the chains are ordered using the same  $l$ -dimensional sort. Different types of sorts are discussed in Section 3.2.

Specifically, we select a deterministic low-discrepancy (QMC) point set of the form  $\tilde{\mathbf{Q}}_n = \{(\mathbf{w}_i, \mathbf{u}_i), i = 0, \dots, n-1\}$ , with  $\mathbf{w}_i \in [0, 1]^l$  and  $\mathbf{u}_i \in [0, 1]^d$ , whose points are already sorted with respect to their first  $l$  coordinates with the multivariate sort that we have selected. At each step  $j$ , we randomize the last  $d$  coordinates of the points of  $\tilde{\mathbf{Q}}_n$  to obtain the RQMC point set

$$\mathbf{Q}_{n,j} = \{(\mathbf{w}_i, \mathbf{U}_{i,j}) : i = 0, \dots, n-1\}, \quad (4)$$

in which each  $\mathbf{U}_{i,j}$  is uniformly distributed in  $[0, 1]^d$ . We also sort the  $n$  states  $\mathbf{X}_{0,j-1}, \dots, \mathbf{X}_{n-1,j-1}$  based on their values of  $h(\mathbf{X}_{0,j-1}), \dots, h(\mathbf{X}_{n-1,j-1})$ , using the same sorting algorithm as for the QMC points, and let  $\pi_j$  denote the permutation of the indices  $\{0, 1, \dots, n-1\}$  implicitly defined by this reordering. Then the  $n$  chains advance to step  $j$  via

$$\mathbf{X}_{i,j} = \varphi(\mathbf{X}_{\pi_j(i),j-1}, \mathbf{U}_{i,j}), \quad i = 0, \dots, n-1.$$

It is also possible to use a different sorting method at each step  $j$ , in which case the QMC points must be sorted differently as well, so this is usually not convenient.

At the end, one computes  $\hat{\mu}_n$  in (3), which is an unbiased estimator of  $\mathbb{E}[g(\mathbf{X}_s)]$ . The main goal of this procedure is for the empirical distribution of the states  $\mathbf{X}_{0,j}, \dots, \mathbf{X}_{n-1,j}$  to better approximate the theoretical distribution of  $\mathbf{X}_j$  at each step  $j$ , than if the chains were simulated independently with standard MC, and as a result reduce the variance of  $\hat{\mu}_n$ . For further theoretical analysis and empirical evidence, see for example L'Ecuyer et al (2008, 2009, 2018). To estimate the variance of this Array-RQMC estimator, one can repeat the entire procedure  $m$  times, with independent randomizations of the points, and take the empirical variance of the  $m$  realizations of  $\hat{\mu}_n$  as an unbiased estimator for  $\text{Var}[\hat{\mu}_n]$ . This Array-RQMC procedure is stated in Algorithm 1.

**Algorithm 1** Array-RQMC Algorithm

---

```

1:  $\mathbf{X}_{i,0} \leftarrow \mathbf{x}_0$  for  $i = 0, \dots, n-1$ ;
2: for  $j = 1, 2, \dots, s$  do
3:   Sort the states  $\mathbf{X}_{0,j-1}, \dots, \mathbf{X}_{n-1,j-1}$  by their values of  $h(\mathbf{X}_{i,j-1})$ ,
4:   using the selected sort, and let  $\pi_j$  be the corresponding permutation;
5:   Randomize afresh the last  $d$  coordinates of the RQMC points,  $\mathbf{U}_{0,j}, \dots, \mathbf{U}_{n-1,j}$ ;
6:   for  $i = 0, 1, \dots, n-1$  do
7:      $\mathbf{X}_{i,j} = \varphi(\mathbf{X}_{\pi_j(i),j-1}, \mathbf{U}_{i,j})$ ;
8:   end for
9: end for
10: Return the estimator  $\hat{\mu}_n = (1/n) \sum_{i=0}^{n-1} g(\mathbf{X}_{i,s})$ .

```

---

## 3.2 Sorting Strategies

In the special case where  $l = 1$ , the RQMC points are sorted by their first coordinate and the states  $\mathbf{X}_{i,j-1}$  are simply sorted by their value of  $h(\mathbf{X}_{i,j-1})$ , in increasing order. In this case, one would typically have  $w_i = i/n$  and the points are already sorted by construction (this is true for all the point sets used in this paper).

When  $\ell > 1$ , sorting for good pairing is less obvious. Two related multivariate sorts that gave good results for other applications are the batch sort and the split sort (Lécot and Coulibaly, 1998; El Haddad et al, 2008; L'Ecuyer et al, 2009, 2018). For the *batch sort* we factor  $n = n_1 n_2 \cdots n_L$  with  $L \geq 1$ . Each time we sort, we split the set of states into  $n_1$  batches of size  $n/n_1$  such that the first coordinate of every state in one batch is smaller or equal to the first coordinate of every state in the next batch; then we further subdivide each batch into  $n_2$  batches of size  $n/(n_1 n_2)$  in the same way but now according to the second coordinate of the states. This procedure is repeated  $L$  times in total. If  $L > \ell$ , after  $\ell$  steps we begin subdividing the batches with respect to their first coordinate again. The *split sort* is simply a variant of the batch sort in which  $n = 2^\ell$  and  $n_1 = n_2 = \dots = n_L = 2$ .

Another way of sorting is to map the states to the  $\ell$ -dimensional unit hypercube  $[0, 1)^\ell$ , so we can assume that the state space is now  $[0, 1)^\ell$  instead of  $\mathbb{N}_0^\ell$ , and then use a discretized version of a space filling curve for this hypercube. The hypercube is partitioned into a grid of small subcubes so that the event that two states fall in the same small subcube has a very small probability, then the states are sorted in the order that their subcubes are visited by the curve (those in the same subcube can be ordered arbitrarily). With this, we use  $(d+1)$ -dimensional RQMC points sorted by their first coordinate. This approach is in fact an implicit way to map the states to the one-dimensional real line, and then use a one-dimensional sort (with  $l = 1$ ). This has been suggested in particular with a Z-curve (Wächter and Keller, 2008) and with a Hilbert curve (Gerber and Chopin, 2015). We call the latter a *Hilbert curve sort*. To map  $\ell$ -dimensional states to  $[0, 1)^\ell$ , Gerber and Chopin (2015) suggest applying a rescaled logistic transformation  $\Psi(x_j) = 1/(1 + \exp[-(x_j - \mu_j + 2\sigma_j)/(4\sigma_j)])$ ,  $1 \leq j \leq \ell$ , to each coordinate. We estimated the means  $\mu_j$  and the variances  $\sigma_j^2$  of the copy numbers of each species at every step, from data obtained from preliminary experiments.

A variant that avoids the need for such a transformation is the *Hilbert batch sort* (L'Ecuyer et al, 2018): One first applies a batch sort to partition  $\mathbb{R}^\ell$  into  $n$  boxes, each of which containing exactly one of the states, then these boxes are associated with  $n$  subcubes in  $[0, 1)^\ell$  and the states are enumerated in the order that the corresponding boxes are visited by the Hilbert curve.

All these multivariate sorts can be computationally expensive when  $n$  is large. For this reason, we made some efforts in this work to explore ways of defining importance functions  $h : \mathbb{N}_0^\ell \rightarrow \mathbb{R}$  that can be computed quickly during the simulations and provide at the same time good representations for the value of a state. An appropriate choice of  $h$  is certainly problem-dependent and good ones have been constructed for some examples in other settings such as computational finance, queueing, and reliability (L'Ecuyer et al, 2007, 2008, 2018; Ben Abdellah et al, 2019).

We adopt the (partly heuristic) idea that at each step  $j$ , an ideal importance function  $h_j$  should have the property that  $h_j(\mathbf{x})$  is a good approximation of  $\mathbb{E}[g(\mathbf{X}_s) \mid \mathbf{X}_j = \mathbf{x}]$  for all  $\mathbf{x} \in \mathbb{N}_0^\ell$  and  $j = 1, \dots, s$  (L'Ecuyer et al, 2007, 2009). To really do this, we would need to construct a different approximation  $h_j$  for each  $j$ . We will call it a *step-dependent importance function* (SDIF). To see how well this general type of approach could perform, we made the following experiment with each of the examples considered in Section 4. First, we generated data by simulating the DTMC for  $n = 2^{20}$  independent ‘‘pilot’’ samples paths, and we collected the  $n$  pairs  $(\mathbf{X}_{i,j}, g(\mathbf{X}_{i,s}))$ ,  $i = 0, \dots, n-1$ , for each  $j$ . Then, our aim was to find a function  $h_j : \mathbb{N}_0^\ell \rightarrow \mathbb{R}$  for which  $h_j(\mathbf{X}_{i,j})$  was a good predictor of  $g(\mathbf{X}_{i,s})$  conditional on  $\mathbf{X}_{i,j}$ . For this, we selected a parameterized form of function  $h_j$ , say  $h_j(\theta, \cdot)$ , which depends on a parameter vector  $\theta$ , and we estimated the best value of  $\theta$  by least-squares regression from the data. The general form that we explored for  $h_j(\theta, \mathbf{x})$  was a linear combination of polynomials in the coordinates of  $\mathbf{x}$ , where  $\theta$  was the vector of coefficients in the linear combination. The motivation for this choice is that the expected number of molecules of a given type at the next step, given the current state, is an affine function of the expected number of reactions of each type that will occur at that step, and this expected number for reaction type  $R_k$  is in turn linear in  $a_k(\mathbf{x})$ , which is a known polynomial in the coordinates of  $\mathbf{x}$ .

A cruder but less expensive strategy uses the same function  $h_j = h$  for all  $j$ . One special case of this is to use  $h_{s-1}$  at all steps. We had some success with this simple version, which we call the *one-step look-ahead importance function* (OSLAIF). In the special case where  $g(\mathbf{x})$  is linear in  $\mathbf{x}$ , say  $g(\mathbf{x}) = \mathbf{b}^t \mathbf{x}$  where  $\mathbf{b}^t$  is the transpose a vector of coefficients, then  $h_{s-1}(\mathbf{x}) \stackrel{\text{def}}{=} \mathbb{E}[g(\mathbf{X}_s) \mid \mathbf{X}_{s-1} = \mathbf{x}] = \mathbb{E}[\mathbf{b}^t \mathbf{X}_1 \mid \mathbf{X}_0 = \mathbf{x}]$  is given by a polynomial in  $\mathbf{x}$ , and one can obtain this polynomial exactly, since

$$\mathbb{E}[\mathbf{X}_1 \mid \mathbf{X}_0 = \mathbf{x}] = \mathbf{x} + \sum_{k=1}^d \zeta_k \mathbb{E}[D_{1,k} \mid \mathbf{X}_0 = \mathbf{x}] = \mathbf{x} + \tau \sum_{k=1}^d \zeta_k a_k(\mathbf{x}), \quad (5)$$

which is a vector of polynomials in  $\mathbf{x}$  that are easy to calculate. This includes the case of  $g(\mathbf{x}) = x_i$ , the number of molecules of species  $i$ , which occurs in all our examples.

Extending this to more than one step can be more difficult when the  $a_k$  are nonlinear. One can write

$$\mathbb{E}[\mathbf{X}_2 \mid \mathbf{X}_0 = \mathbf{x}] = \mathbf{x} + \tau \sum_{k=1}^d \zeta_k [a_k(\mathbf{x}) + \mathbb{E}[a_k(\mathbf{X}_1) \mid \mathbf{X}_0 = \mathbf{x}]],$$

but when  $a_k$  is nonlinear, the quantity in the last expectation is a nonlinear function of a random vector. Extending to more steps leads to even more complicated embedded conditional expectations. This motivated us to try just the OSLAIF rule as a heuristic, and we got some good results with that. Specific illustrations are given in Section 4.

Let  $\tilde{h}_j$  denote the functions  $h_j$  estimated from data as just described, for each  $j$ . These  $\tilde{h}_j$  are noisy estimates, and since they are estimated separately across values of  $j$ , we can



observe some random variation when looking at their sequence as a function of  $j$ . To smooth out this variation, we tried fitting a (least-squares) smoothing spline (de Boor, 2001; Pollock, 1993) to this sequence of functions  $\tilde{h}_j$  to obtain a sequence of functions  $h_j$ ,  $j = 1, \dots, s$ , that varies more smoothly across the step number  $j$ . This yields a *smoothed SDIF*. In our experiments, we never observed a large improvement by doing this, because with  $n = 2^{20}$  pilot simulations, the  $\tilde{h}_j$  did not vary much already as a function of  $j$ . But the smoothing might be worthwhile when the number  $n$  of pilot simulations is smaller.

### 3.3 RQMC Point Sets

The RQMC point sets considered in this paper are the following (the short names in parentheses are used to identify them in the next section): (1) a randomly-shifted rank-1 lattice rule (Lat+s); (2) a Lat+s with the baker's transformation applied to the points after the shift (Lat+s+b); (3) a Sobol' net with a left random matrix scramble followed by a random digital shift (Sob+LMS); (4) a Sobol' net with the nested uniform scramble of Owen (1997) (Sob+NUS). These point sets and randomizations are defined and explained in L'Ecuyer and Lemieux (2000); Owen (2003); L'Ecuyer (2009, 2018). They are implemented in SSJ (L'Ecuyer and Buist, 2005; L'Ecuyer, 2016), which we used for all our experiments. For the lattice rules, the parameters were found with the Lattice Builder tool (L'Ecuyer and Munger, 2016), using the weighted  $\mathcal{P}_2$  criterion with order dependent weights equal to  $\rho^k$  for each projection of order  $k$ , for each  $k$ , with  $\rho = 0.6$  for Example 4.1 and for the PKAr case in Example 4.3 (the small-dimensional cases), and  $\rho = 0.05$  in all the other cases. The baker's transformation stretches each coordinate of each point by a factor of 2, then folds back the values by replacing  $u$  with  $2 - u$  when  $u > 1$ . This is equivalent to transforming the integrand to make it periodic, which may improve the convergence rate (Hickernell, 2002) and may provide huge improvements in some cases, but it also increases the variation of the integrand, so it may increase the variance (moderately) in other cases. For the Sobol' points, we used the parameters (direction numbers) from Joe and Kuo (2008), except for Example 4.1 and the PKAr case in Example 4.3, for which we used the parameters from Lemieux et al (2004).

## 4 Numerical Illustrations

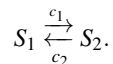
For our numerical illustrations, we use two low-dimensional examples taken from Beentjes and Baker (2019), then a higher-dimensional example from Padgett and Ilie (2016). On these examples, we compare the performances of both classical RQMC and Array-RQMC in combination with  $\tau$ -leaping. All experiments were run using SSJ (L'Ecuyer and Buist, 2005; L'Ecuyer, 2016), which provides the required RQMC tools and also implements the sorting methods discussed in Section 3.2. The MRG32k3a random number generator was used for MC and all the randomizations.

We repeated each Array-RQMC procedure  $m = 100$  times independently to estimate the RQMC variance  $\text{Var}[\hat{\mu}_n]$  for  $n = 2^{13}, \dots, 2^{19}$ . We then fitted a model of the form  $\text{Var}[\hat{\mu}_n] \approx \kappa n^{-\beta}$  to these observations by least-squares linear regression in log-log scale. This gave an estimated convergence rate of  $\mathcal{O}(n^{-\hat{\beta}})$  for the variance, where  $\hat{\beta}$  is the least-square estimate of  $\beta$ . We report this  $\hat{\beta}$  in our results. Ordinary MC gives  $\beta = 1$ , so we can compare. We also provide a few plots of  $\text{Var}[\hat{\mu}_n]$  as a function of  $n$ , in log-log scale, to illustrate the typical behavior. Our logs are always in base 2, because we always use powers of 2 for  $n$ .

We computed the estimated *variance reduction factor* (VRF) of Array-RQMC compared with MC, which is defined as  $\text{Var}[g(\mathbf{X}_s)]/(n\text{Var}[\hat{\mu}_n])$  where  $\text{Var}[g(\mathbf{X}_s)]$  is the MC variance for a single run, which was estimated separately by making  $n = 10^6$  independent runs. This is the variance per run for MC divided by the variance per run for Array-RQMC. We call VRF19 this value for  $n = 2^{19}$  and we report it in our results. We also computed an *efficiency ratio* which measures the change in the work-normalized variance (the product of the estimator’s variance by its computing cost). It is the VRF multiplied by the CPU time required to compute  $n$  realizations with MC and divided by the CPU time to compute the RQMC or Array-RQMC estimator with the same  $n$ . We call EIF19 its value for  $n = 2^{19}$  and we report it as well. This measure takes into account both the gain in variance and the extra cost in CPU time which is required to sort the chains at each step of the Array-RQMC algorithm. Note that using RQMC only is generally not slower than MC, but usually a bit faster.

#### 4.1 A Reversible Isomerization System

We start with the same simple model of a *reversible isomerization system* as Beentjes and Baker (2019). There are two species,  $S_1$  and  $S_2$ , and  $d = 2$  reaction channels with reaction rates  $c_1 = 1$  and  $c_2 = 10^{-4}$ :



We start with  $X_1(0) = 10^2$  molecules of type  $S_1$  and  $X_2(0) = 10^6$  molecules of type  $S_2$ . Since the total number of molecules is constant over time, it suffices to know the number of molecules of the first type,  $X_1(t)$ , at any time  $t$ , so we can define the state of the CTMC as  $\mathbf{X}(t) = X_1(t)$  only. This gives us  $\ell = 1$ . Then, we only need a one-dimensional sort for Array-RQMC. We also take  $g(\mathbf{X}(t)) = X_1(t)$ . Note that with our choice of initial state,  $\mathbb{E}[X_1(t)] = 10^2$  for all  $t > 0$ , so we already know the answer for this simple example. There are two possible reactions, so  $d = 2$ , and we therefore need RQMC points in  $2s$  dimensions with classical RQMC and in  $\ell + d = 3$  dimensions with Array-RQMC.

Table 1 summarizes our experimental results. Seven cases are reported in the table. The first case (in the upper left) has the same parameters as Beentjes and Baker (2019):  $T = 1.6$ , and  $s = 8$ , so  $\tau = T/s = 0.2$ . Figure 1 displays how the variance decreases as a function of  $n$  for this case. Notice the steeper slope for the four Array-RQMC variants. Array-RQMC clearly outperforms both MC and classical RQMC in this example.

We also observe with these three cases that when we increase  $s$  with  $T$  fixed, the factors VRF19 and EIF19 diminish, and the diminution is much more prominent with RQMC. The latter might be no surprise, because increasing  $s$  increases the dimension of the RQMC points. But it was unclear a priori if it would also occur with Array-RQMC, and how much. However, by doing further experimentation, we found that the decrease of VRF19 is not really due to the increase in the number of steps, but rather to the decrease in  $\tau$ . To see that, look at the fourth case, with  $(T, s, \tau) = (25.6, 128, 0.2)$ . Here we have the same  $\tau$  as in the first case, but  $s$  is multiplied by 16. For the Array-RQMC methods, the variance reductions and convergence rates are similar to the first case. For RQMC, they are a bit lower, which is not surprising because the dimension has increased. For cases five and six, we have increased  $\tau$  to 0.8 and we compare two large values of  $s$ . The VRF19’s are roughly comparable, which means that they really depend on  $\tau$  and not much on  $s$ . Why is that?

Recall that in this example, at each step we generate a pair of Poisson random variables, which are discrete and therefore discontinuous with respect to the underlying uniforms. The

Table 1: Estimated rates  $\hat{\beta}$ , VRF19, and EIF19, for the reversible isomerization example, for various choices of  $(T, s, \tau)$ . MC refers to ordinary MC, RQMC is classical RQMC with Sobol' points and LMS randomization, and the other four rows are for Array-RQMC with different RQMC point sets. "MC Var" is  $\text{Var}[g(\mathbf{X}_s)]$ , the variance per run with MC.

$(T, s, \tau) \rightarrow$	(1.6, 8, 0.2)			(1.6, 128, 0.2/16)			(1.6, 1024, 0.2/128)		
MC Var	107.8			96.6			96.0		
Point sets	$\hat{\beta}$	VRF19	EIF19	$\hat{\beta}$	VRF19	EIF19	$\hat{\beta}$	VRF19	EIF19
MC	1.00	1	1	1.00	1	1	1.00	1	1
RQMC	1.03	629	1,493	1.08	79	83	1.01	46	68
Lat+s	1.81	27,864	14,835	1.82	17,163	5,315	1.64	6,918	2,098
Lat+s+b	1.60	14,420	7,636	1.74	6,133	1,838	1.53	1,997	553
Sob+LMS	1.64	18,892	9,819	1.62	8,370	2,785	1.57	3,949	1,386
Sob+NUS	1.70	17,518	6,440	1.60	5,773	1,095	1.65	3,182	667

$(T, s, \tau) \rightarrow$	(25.6, 128, 0.2)			(102.4, 128, 0.8)			(819.2, 1024, 0.8)		
MC Var	111.0			166.7			166.6		
Point sets	$\hat{\beta}$	VRF19	EIF19	$\hat{\beta}$	VRF19	EIF19	$\hat{\beta}$	VRF19	EIF19
MC	1.00	1	1	1.00	1	1	1.00	1	1
RQMC	1.06	519	625	1.10	2,294	2,381	1.12	2,887	3,018
Lat+s	1.78	21,084	11,030	1.83	32,538	23,379	1.81	31,909	23,372
Lat+s+b	1.80	26,566	13,666	1.72	45,841	33,229	1.66	47,264	35,627
Sob+LMS	1.62	17,358	9,290	1.66	46,883	32,813	1.49	32,220	23,094
Sob+NUS	1.61	15,624	6,044	1.57	40,161	23,552	1.53	30,970	17,123

$(T, s, \tau) \rightarrow$	(1.6, 8, 0.2), normal		
MC Var	107.8		
Point sets	$\hat{\beta}$	VRF19	EIF19
MC	1.00	1	1
RQMC	1.94	3,673,231	5,484,012
Lat+s	1.89	56,401	9,160
Lat+s+b	2.00	185,153,839	29,679,837
Sob+LMS	2.03	4,118,783	664,232
Sob+NUS	2.01	4,658,933	541,339

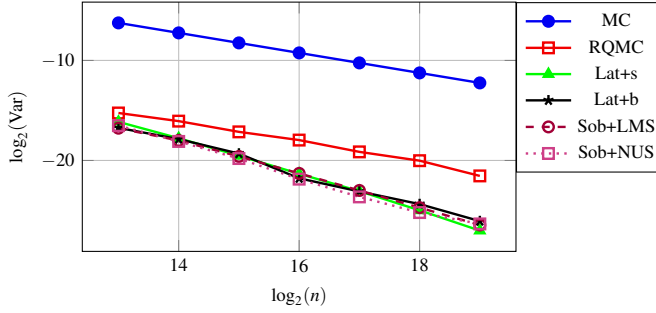


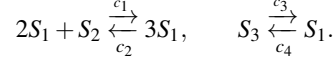
Fig. 1: Estimated  $\text{Var}[\hat{\mu}_n]$  as a function of  $n$ , in log-log scale, for the reversible isomerization system, with  $T = 1.6$  and  $s = 8$ .

mean of each Poisson random variable is proportional to  $\tau$ , and the larger the mean, the closer it is to a continuous distribution. In fact, as  $\tau$  increases, the Poisson converges to a normal distribution, whose inverse cdf is smooth, so the generated values are smooth functions of the underlying uniforms in the limit. That is, we obtain a better VRF19 when  $\tau$  is larger because the integrand is closer to a continuous (and smooth) function. When the Poisson distributions have small means, in contrast, the response has larger discontinuities. And it is well known that RQMC is much more effective for smooth functions than discontinuous functions. This kind of behavior was already pointed out for RQMC in Section 5.2 of Beentjes and Baker (2019). Interestingly, we see that the same effect applies to Array-RQMC as well. To illustrate this effect “in the limit,” we made an experiment in which all the Poisson random variables at each step are replaced by normals with the same mean and variance, and the state vector has real-valued components rather than integer components, using the same parameters as in the first case in the table. The results are in the last (bottom) entry of the table and they are stunning. Firstly, for RQMC and all Array-RQMC methods, the rate  $\beta$  is close to 2, which does not occur for the other cases. Secondly, the VRF19 factor is also very large for RQMC and is huge in particular for Array-RQMC with Lat+s+b. This surprising result for RQMC can be explained as follows. Here the integrand has 16 dimensions, but on a closer look one can see that it is a sum of 16 normal random variables that are almost independent; i.e., almost a sum of one-dimensional functions. This means that the effective dimension is close to 1, and this explains the success of RQMC. Regarding the huge gain with Lat+s+b, it can be explained by the fact that for a smooth one-dimensional function, RQMC with Lat+s+b can provide an  $\mathcal{O}(n^{-4})$  convergence rate for the variance (Hickernell, 2002; L’Ecuyer, 2009). Essentially, for one-dimensional smooth functions, the baker’s transformation produces a locally antithetic effect which integrates exactly the piecewise linear approximation, and only higher-order error terms remain. The huge VRF19 indicates that part of this effect carries over to Array-RQMC.

We just saw that as a rough rule of thumb, the RQMC methods bring more gain when the Poisson random variables have larger means. We know (from Section 2) that the mean of the Poisson random variable  $D_{j,k}$  is  $a_k(\mathbf{X}_{j-1})\tau$ . This mean can be increased by increasing either  $\tau$  or the components of the state vector. For the present example, if we denote  $\mathbf{X}_{j-1} = (X_{j-1}^{(1)}, X_{j-1}^{(2)})^\top$ , the number of molecules of each of the two types at step  $j-1$ , we have  $a_k(\mathbf{X}_{j-1}) = c_k X_{j-1}^{(k)}$  for  $k = 1, 2$ , so the Poisson means are increased by a factor  $\gamma > 1$  by either multiplying  $\tau$  by  $\gamma$  or multiplying the vector  $\mathbf{X}_{j-1}$  by  $\gamma$ . We made experiments whose results agreed with that when all the components of the state were large enough. But if one component of  $\mathbf{X}_{j-1}$  is small, and we increase  $\tau$  and simulate the system over a few steps, this component has a good chance of getting close to zero at some step, and this increases the discontinuity. In that situation, a larger  $\tau$  can worsen the VRF. To further test the above reasoning, we made another set of experiments in which the initial state  $\mathbf{X}_0$  had two equal components, exactly  $X_0^{(1)} = X_0^{(2)} = (10^2 + 10^6)/2$  molecules of each type, and we adapted the reaction rates to  $c_1 = c_2 = 100/X_0^{(1)}$ , to keep  $\mathbb{E}[X_1(t)] = X_0^{(1)}$  for all  $t$ . In this case, the problem of one component getting close to 0 does not occur so things remain smoother. We found that the VRFs were larger than in Table 1 for both RQMC and Array-RQMC (we exclude the normal distribution). The VRF for RQMC was also smaller when both  $T$  and  $s$  were large, but not when  $s$  was increased and  $T$  remained small. One possible explanation for this is that when  $T$  and  $s$  are large, the overall change in the state can be large, and then the set of successive changes in the state are less independent, which increases the effective dimension.

#### 4.2 The Schlögl System

In this second example, also taken from Beentjes and Baker (2019), we have the three species  $S_1$ ,  $S_2$  and  $S_3$ , and four reaction channels with reaction rates  $c_1 = 3 \times 10^{-7}$ ,  $c_2 = 10^{-4}$ ,  $c_3 = 10^{-3}$  and  $c_4 = 3.5$ , respectively. The model can be depicted as:



The propensity functions  $a_k$  are given by

$$\begin{aligned} a_1(\mathbf{x}) &= c_1 x_1 (x_1 - 1) x_2 / 2, & a_2(\mathbf{x}) &= c_2 x_1 (x_1 - 1) (x_1 - 2) / 6, \\ a_3(\mathbf{x}) &= c_3 x_3, & a_4(\mathbf{x}) &= c_4 x_1. \end{aligned}$$

We also take  $\mathbf{x}_0 = (250, 10^5, 2 \times 10^5)^t$ ,  $T = 4$ , and  $\tau = T/16$ , so  $s = 16$  steps. This the same model as in Beentjes and Baker (2019), with the same parameters, except that we took a smaller  $\tau$  to avoid negative copy numbers. We want to estimate  $\mathbb{E}[X_1(T)]$ , the expected number of molecules of  $S_1$  at time  $T$ . Here, this expectation does depend on  $T$ , and we will see that  $\text{Var}[X_1(T)]$  also depends very much on  $T$ .

Since the total number of molecules remains constant over time, the dimension of the state here can be taken as  $\ell = 2$ . We take the state as  $\mathbf{X} = (X^{(1)}, X^{(2)})^t$ , and  $X^{(3)}$  can be deduced by  $X^{(3)} = N_0 - X^{(1)} - X^{(2)}$  where  $N_0$  is the total number of molecules. With  $d = 4$  possible reactions, the RQMC points must be five-dimensional if we construct an importance function  $h$  that maps the state to one dimension, and must be six-dimensional otherwise. For comparison, with classical RQMC, the dimension of the RQMC points is  $d[T/\tau] = 64$ .

In the previous example, the state was one-dimensional, so there was no need to define an importance function for Array-RQMC, but here we have a two-dimensional state. We now examine how to construct an importance function  $h_j : \mathbb{N}_0^2 \rightarrow \mathbb{R}$  as discussed in Section 3.2. To construct an importance function  $h : \mathbb{N}_0^2 \rightarrow \mathbb{R}$  using the OSLAIF, when  $g(\mathbf{x})$  is a linear function of  $\mathbf{x}$ , one can compute the conditional expectation *exactly* by using by (5). This gives a polynomial of the form:

$$h_j(x_1, x_2) = \theta_0 + \theta_1 x_1 + \theta_2 x_2 + \theta_3 x_1^2 + \theta_4 x_1 x_2 + \theta_5 x_1^3 + \theta_6 x_1^2 x_2. \quad (6)$$

With  $g(\mathbf{x}) = x_1$  (our case), the coefficients are  $(\theta_0, \theta_1, \dots, \theta_6) \approx (300.25\tau, 1 - 3.5\tau, -10^{-3}\tau, 5 \times 10^{-5}\tau, -1.5 \times 10^{-7}\tau, -1.67 \times 10^{-5}\tau, 1.5 \times 10^{-7}\tau)$ . If  $x_1$  was very large, we could approximate  $a_1(\mathbf{x}) \approx c_1 x_1^2 x_2 / 2$  and  $a_2(\mathbf{x}) = c_2 x_1^3 / 6$ , and then remove the two terms  $\theta_3 x_1^2 + \theta_4 x_1 x_2$  from (6), but in our example,  $x_1$  is not very large.

To obtain a SDIF for a more general  $j$ , one possible heuristic could be to assume the same form of polynomial (even if this is not exact) and select the coefficients  $\theta_i$  by least-squares fitting to data obtained from  $n = 2^{19}$  pilot runs as explained in Section 3.2. We did this and we also tried fitting a more general bivariate polynomial that contains all possible monomials  $x^{\epsilon_1} y^{\epsilon_2}$  with  $0 \leq \epsilon_1, \epsilon_2 \leq 3$ , but this gave us no improvement over OSLAIF. The other SDIF approaches that we tried also did no better than OSLAIF. A plausible explanation is that the functions  $h_j$  in this case are based on data obtained from noisy simulations (large variance and dependence on  $j$ ). A possible alternative could be to use automatic learning with a deep neural network to learn a good  $h$ . But this is beyond our scope.

For the batch sort, we kept the three coordinates in their natural order and we used  $n_1 = \lceil n^{1/2} \rceil$  and  $n_2 = \lceil (n/n_1)^{1/2} \rceil$ . For  $n = 2^{19}$ , for example, this gives  $n_1 = 725$  and  $n_2 = 27$ .

Table 2 summarizes our experimental results with this example. Array-RQMC performs much better than RQMC. It reduces the variance by factors in the thousands, and over 8,000

in one case with  $n = 2^{19}$ . The OSLAIF, Hilbert curve sort, and batch sort all perform reasonably well, which is not very surprising, because the state space is only two-dimensional. The OSLAIF is very effective for  $T = 4$ , but somewhat less effective for  $T = 32$ . Globally, the batch sort is the best performer; its VRF19 and EIF19 values are both consistently among the largest ones. The Sobol' points are generally the best performers for each type of sort.

The left panel of Figure 2 shows  $\text{Var}[\hat{\mu}_n]$  versus  $n$  in log-log scale for the OSLAIF sort, for various point sets. The estimated convergence rates  $-\hat{\beta}$  are mostly between -1.3 and -1.6, which clearly beats the usual MC rate of -1. The right panel shows  $\text{Var}[\hat{\mu}_n]$  as a function of  $n$  under Sob+LMS, in a log-log-scale.

One important observation is the large difference in MC variance between  $T = 4$  and  $T = 32$ ; it is larger at  $T = 4$  by a factor of about 100. The mean  $\mathbb{E}[\hat{\mu}_n]$  also depends on  $T$ : it is about 240 at  $T = 4$  and about 86 at  $T = 32$ . It is plotted as a function of  $T$  in the left panel of Figure 3. What happens is that the trajectories have roughly two very different kinds of transient regimes between  $t = 0$  and about  $t = 10$ . For some trajectories,  $X_1(t)$  goes up to somewhere between 400 and 600 at around  $t = 4$ , then goes down to around the long-term mean, say between 70 and 100. For other trajectories,  $X_1(t)$  decreases right away to between 70 and 100 at around  $t = 5$ . Figure 3 illustrates this behavior, with 16 sample paths. This was already mentioned in Beentjes and Baker (2019), although they say the system is bistable, whereas what we observe is rather two types of *transient* paths. This behavior explains the much larger variance at  $T = 4$  than at  $T = 32$ . It also shows why it is very hard to predict the state at some larger  $T$  from the state at  $t = 1/4$ , say, hence the difficulty to estimate an ‘‘optimal’’ importance function. Despite all of this, Array-RQMC performs quite well with simple sorts and brings large efficiency improvements compared with MC and RQMC.

Table 2: Estimated rates  $\hat{\beta}$ , VRF19, and EIF19 for the Schlögl system, with various types of sorts for Array-RQMC.

		$T = 4, s = 16$			$T = 4, s = 128$			$T = 32, s = 128$		
MC Var		27,409			27,471			270		
Sort	Sample	$\hat{\beta}$	VRF19	EIF19	$\hat{\beta}$	VRF19	EIF19	$\hat{\beta}$	VRF19	EIF19
	MC	1.00	1	1	1.00	1	1	1.00	1	1
	RQMC	1.14	11	12	1.04	7	8	1.29	211	203
OSLAIF	Lat+s	1.55	1814	1051	1.49	2072	1403	1.23	508	541
	Lat+s+b	1.26	4375	2567	1.38	1230	861	1.08	471	506
	Sob+LMS	1.37	6133	3775	1.46	3112	2285	1.11	556	629
	Sob+NUS	1.33	5254	2813	1.49	3258	1556	1.13	461	483
Batch	Lat+s	1.62	2979	2657	1.58	2150	830	1.47	2136	2259
	Lat+s+b	1.39	4831	2650	1.39	1123	415	1.34	1682	1791
	Sob+LMS	1.54	8147	4880	1.46	2202	1503	1.26	1614	1274
	Sob+NUS	1.44	5761	3007	1.42	2024	1102	1.26	1483	989
Hilbert	Lat+s	1.46	509	419	1.41	652	350	1.33	837	614
	Lat+s+b	1.49	1468	1213	1.18	375	216	1.28	1159	848
	Sob+LMS	1.58	3604	1973	1.29	575	313	1.25	1642	1231
	Sob+NUS	1.58	3183	1657	1.28	617	255	1.28	1358	881

### 4.3 A model of cyclic adenosine monophosphate activation of protein kinase A

This example is a model for the cyclic adenosine monophosphate (cAMP) activation of protein kinase A (PKA), taken from Koh and Blackwell (2012) and Strehl and Ilie (2015).

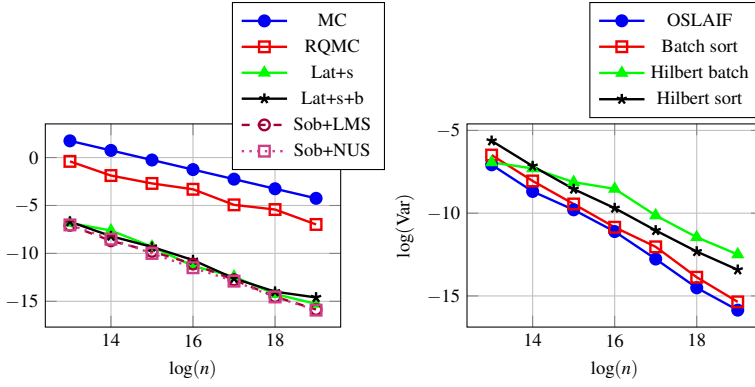


Fig. 2: Empirical variance of the sorting methods vs  $n$  in a log-log scale,  $T = 4$ ,  $s = 128$ , for the OSLAIF sort and various point sets (left) and for various sorts with Sobol+LMS (right).

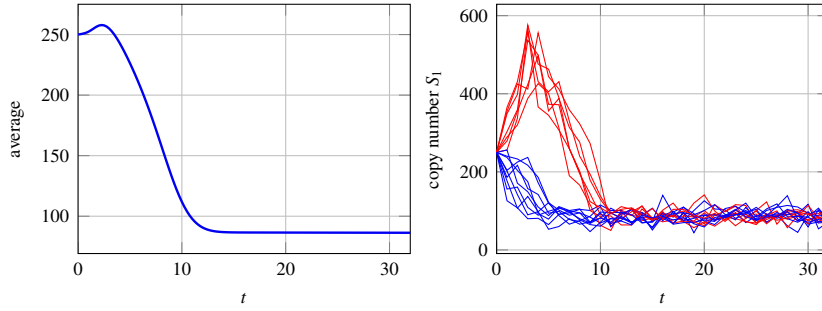
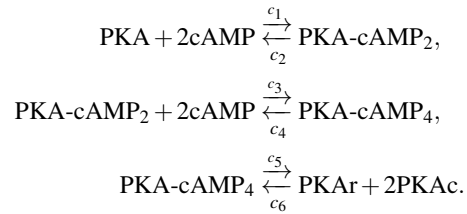


Fig. 3: The mean with  $n = 2^{19}$  (left) and the trajectories of  $X_1(t)$  for  $n = 16$  chains for  $t \leq 32$  (right).

This model is interesting because it has  $\ell = 6$  and  $d = 6$ , which are both larger than in the previous examples. The six molecular species  $S_1$  to  $S_6$  are (in this order) PKA, cAMP, the partially saturated PKA-cAMP<sub>2</sub>, the saturated PKA-cAMP<sub>4</sub>, the catalytic subunit PKAr, and the regulatory subunit PKAc. The  $d = 6$  possible reactions are depicted here:



The reaction rates are  $c_1 = 2.6255 \times 10^{-6}$ ,  $c_2 = 0.02$ ,  $c_3 = 3.8481 \times 10^{-6}$ ,  $c_4 = 0.02$ ,  $c_5 = 0.016$  and  $c_6 = 5.1325 \times 10^{-5}$ . We simulate this system with the same parameters as Padgett and Ilie (2016), except that we assume that the molecules are homogeneously distributed in the volume and we choose a fixed  $\tau$  as opposed to selecting it adaptively after each step. At time zero there are 33,000 molecules of PKA, 33,030 molecules of cAMP, and

1, 100 molecules of each other species. We take  $T = 0.05$  and  $\tau = T/256$ , so  $s = 256$  steps. This problem requires RQMC points in 7 or 12 dimensions with Array-RQMC, compared with 1536 dimensions with classical RQMC.

We report experiments with two different objective functions. The first one is  $\mathbb{E}[X_1(T)]$ , the expected number of molecules of PKA at time  $T$ , and the second one is  $\mathbb{E}[X_5(T)]$ , the expected number of molecules of PKAr at time  $T$ . In each case, we implemented and tested the OSLAIF and SDIF methods to select a mapping  $h$  to one dimension. We also tried the multivariate batch and split sorts, the Hilbert sort, and the Hilbert batch sort, from Section 3.2. The best performers were the OSLAIF map, the batch sort, and the Hilbert sort.

The OSLAIF in this case is given by the polynomial  $h(\mathbf{x}) = x_1 + \tau(-c_1x_1x_2(x_2 - 1)/2 + c_2x_3)$ . In this function, the magnitude  $x_1$  outweighs that of the  $-\tau c_1x_1x_2(x_2 - 1)/2$  term on average, followed by  $\tau c_2x_3$ . This suggests taking  $x_1$  as the most important coordinate for the sort, followed by  $x_2$  and  $x_3$ . So for the batch sort, we used the three coordinates  $x_1, x_2, x_3$  in this order. We tried a few settings for the batch sizes and ended up with  $n_1 = \lceil n^{1/2} \rceil$ ,  $n_2 = \lceil (n/n_1)^{3/8} \rceil$ , and  $n_3 = \lceil (n/n_1/n_2)^{1/8} \rceil$ . For  $n = 2^{19}$ , this gives  $n_1 = 725$ ,  $n_2 = 12$ , and  $n_3 = 2$ .

Table 3 summarizes our results for the PKA case, for which  $g(\mathbf{x}) = x_1$ . The estimated mean and variance per run are also 19663 and 1775, respectively. We find that the three sorting methods reported in the table offer comparable performance in terms of VRF19, although OSLAIF and the batch sort dominate when we look at the EIF19. This is because sorting on a single value or a restricted set of coordinates, as we do for the batch sort, is faster than a full multivariate sort. Classical RQMC also performs surprisingly well despite the large number of dimensions, but not as well as Array-RQMC with the best sorts. With Array-RQMC, we also observe empirical convergence rates  $\hat{\beta}$  consistently better than the MC rate of 1.0. This indicates that the VRF should increase further with  $n$ .

Table 4 gives the results for the PKAr case, for which  $g(\mathbf{x}) = x_5$ . The estimated mean and variance per run are about 716 and 47, respectively. For this case, the OSLAIF is given by  $h(\mathbf{x}) = x_5 + \tau(c_5x_4 - 0.5c_6x_5x_6(x_6 - 1))$ . Given that  $x_4, x_5$ , and  $x_6$  remain roughly between 500 and 1000 in this model, and that  $\tau = 1/5120$ , the dominating term in this function is (by far)  $x_5$ , followed by  $-\tau c_6x_5x_6^2 \approx -2.5 \times 10^{-3}x_5$ . Based on this, for the batch sort, we initially used the coordinates  $x_5, x_6, x_4$  in this order, and took  $n_1 = \lceil n^{1/2} \rceil$ ,  $n_2 = \lceil (n/n_1)^{3/8} \rceil$ , and  $n_3 = \lceil (n/n_1/n_2)^{1/8} \rceil$  for the batch sizes, as in the previous case. This is denoted by ‘‘Batch-5’’ in the table.

We also tried SDIF with various types of functions, but it did not really perform better. While doing that, we applied the random forest permutation-based statistical procedure of Breiman (2001) to detect the most important variables in a noisy function. This procedure told us that  $x_6$  was by far the most important variable for the sort, at all steps. Based on this, we also tried a batch sort with the three coordinates  $x_6, x_5, x_4$  in this order, with the same batch sizes as before. This is named ‘‘Batch-6’’ in the table. We also tried sorting the states by  $x_6$  (the number of PKAc molecules) only. This is a degenerate form of batch sort with  $n_1 = n$ . We call it ‘‘By PKAc’’ in Table 4.

The OSLAIF, Batch-6, and ‘‘By PKAc’’ sorts perform similarly. They provide large improvement factors for both the variance and the efficiency, and empirical convergence rates  $\hat{\beta}$  that are significantly larger than 1. Their performance is orders of magnitude better than RQMC. The Batch-5 and Hilbert sorts are not competitive with the other ones in this case, but they nevertheless reduce the variance by significant factors.

This example illustrates two facts. First, the dimension of the state is not the ultimate criterion for Array-RQMC to perform well. Secondly, customizing sorting algorithms based on information on the underlying model can improve results significantly.



Table 3: Estimated rates  $\hat{\beta}$ , VRF19, and EIF19, for PKA with  $T = 0.05$ ,  $s = 256$ .

Sort	Sample	$\hat{\beta}$	VRF19	EIF19
	MC	1.00	1	1
	RQMC	1.08	464	603
OSLAIF	Lat+s	1.50	1420	806
	Lat+s+b	1.26	745	423
	Sob+LMS	1.29	1295	937
	Sob+NUS	1.29	1174	480
Batch	Lat+s	1.43	1163	567
	Lat+s+b	1.25	1264	604
	Sob+LMS	1.15	1699	981
	Sob+NUS	1.22	1633	353
Hilbert	Lat+s	1.27	1181	452
	Lat+s+b	1.06	821	280
	Sob+LMS	1.15	850	327
	Sob+NUS	1.24	1217	266

Table 4: Estimated rates  $\hat{\beta}$ , VRF19, and EIF19, for PKAr with  $T = 0.05$ ,  $s = 256$ .

Sort	Sample	$\hat{\beta}$	VRF19	EIF19
	MC	1.03	1	1
	RQMC	1.17	39	45
By PKAc	Lat+s	1.33	2470	1585
	Lat+s+b	1.36	1364	1248
	Sob+LMS	1.45	1856	1580
	Sob+NUS	1.50	2053	668
OSLAIF	Lat+s	1.42	3634	1550
	Lat+s+b	1.38	1491	627
	Sob+LMS	1.47	2062	1059
	Sob+NUS	1.51	2184	712
Batch-5	Lat+s	1.48	225	116
	Lat+s+b	1.49	406	203
	Sob+LMS	1.43	576	366
	Sob+NUS	1.37	668	180
Batch-6	Lat+s	1.62	3026	1560
	Lat+s+b	1.43	1592	796
	Sob+LMS	1.46	2753	1749
	Sob+NUS	1.47	2486	670
Hilbert	Lat+s	1.17	135	54
	Lat+s+b	1.12	88	27
	Sob+LMS	1.24	126	60
	Sob+NUS	1.22	161	50

## 5 Conclusion

We have studied the combination of the fixed step  $\tau$ -leap algorithm with Array-RQMC for well-mixed chemical reaction networks and found that in this way, we can reduce the variance in comparison to MC significantly. In contrast to the simulation with traditional RQMC, this approach could often also improve the convergence rate of the variance. Array-RQMC requires to sort the chains by their states at each step of the chain. This can be done with a multivariate sort, which may become costly when the state space has large dimensionality. But we also showed that one can construct sorts by mapping the states into the real numbers by an uncomplicated importance function, where sorting is trivial. A simple variant named OSLAIF performs comparably as well or better than several standard sorting

algorithms, while being naturally easier and less costly to apply. We have also shown that obtaining additional knowledge of the model, such as identifying important variable projections, and adapting a sort to this information can improve the convergence of the variance tremendously.

**Acknowledgements** This work has been supported by a Canada Research Chair, an IVADO Research Grant, and an NSERC Discovery Grant number RGPIN-110050 to P. L'Ecuyer. F. Puchhammer was also supported by Spanish and Basque governments fundings through BCAM (ERDF, ESF, SEV-2017-0718, PID2019-108111RB-I00, PID2019-104927GB-C22, BERC 2018e2021, EXP. 2019/00432, ELKARTEK KK-2020/00049), and the computing infrastructure of i2BASQUE academic network and IZO-SGI SGIker (UPV).

## References

- Anderson D, Higham D (2012) Multilevel Monte Carlo for continuous-time Markov chains, with applications in biochemical kinetics. *Multiscale Modeling & Simulation* 10(1):146–179, DOI 10.1137/110840546
- Anderson DF (2008) Incorporating postleap checks in tau-leaping. *The Journal of Chemical Physics* 128(5):054,103, URL <https://doi.org/10.1063/1.2819665>
- Anderson DF, Kurtz TG (2011) Continuous time Markov chain models for chemical reaction networks. In: Koeppl H, Densmore D, Setti G, di Bernardo M (eds) *Design and analysis of biomolecular circuits*, vol 117, Springer, New York, pp 3–42
- Anderson WJ (1991) *Continuous-Time Markov Chains: An Applications-Oriented Approach*. Springer-Verlag, New York
- Beentjes CHL, Baker RE (2019) Quasi-Monte Carlo methods applied to tau-leaping in stochastic biological systems. *Bulletin of Mathematical Biology* 81:2931–2959
- Ben Abdellah A, L'Ecuyer P, Puchhammer F (2019) Array-RQMC for option pricing under stochastic volatility models. In: *Proceedings of the 2019 Winter Simulation Conference*, IEEE Press, pp 440–451
- Breiman L (2001) Random forests. *Machine learning* 45(1):5–32
- de Boor C (2001) *A Practical Guide to Splines*, 2nd edn. Springer-Verlag, New York
- Demers V, L'Ecuyer P, Tuffin B (2005) A combination of randomized quasi-Monte Carlo with splitting for rare-event simulation. In: *Proceedings of the 2005 European Simulation and Modeling Conference, EUROSIS*, Ghent, Belgium, pp 25–32
- Dick J, Pillichshammer F (2010) *Digital Nets and Sequences: Discrepancy Theory and Quasi-Monte Carlo Integration*. Cambridge University Press, Cambridge, U.K.
- Dion M, L'Ecuyer P (2010) American option pricing with randomized quasi-Monte Carlo simulations. In: *Proceedings of the 2010 Winter Simulation Conference*, pp 2705–2720
- El Haddad R, Lécot C, L'Ecuyer P (2008) Quasi-Monte Carlo simulation of discrete-time Markov chains on multidimensional state spaces. In: Keller A, Heinrich S, Niederreiter H (eds) *Monte Carlo and Quasi-Monte Carlo Methods 2006*, Springer-Verlag, Berlin, pp 413–429
- Fox BL, Glynn PW (1990) Discrete-time conversion for simulating finite-horizon Markov processes. *SIAM Journal on Applied Mathematics* 50:1457–1473
- Gerber M, Chopin N (2015) Sequential quasi-Monte Carlo. *Journal of the Royal Statistical Society, Series B* 77(Part 3):509–579
- Giles MB (2016) Algorithm 955: approximation of the inverse Poisson cumulative distribution. *ACM Transactions on Mathematical Software* 42:1–22
- Gillespie DT (1977) Exact stochastic simulation of coupled chemical reactions. *The Journal of Physical Chemistry* 81(25):2340–2361, DOI 10.1021/j100540a008

- Gillespie DT (2000) The chemical Langevin equation. *The Journal of Chemical Physics* 113(1):297–306
- Gillespie DT (2001) Approximate accelerated stochastic simulation of chemically reacting systems. *The Journal of Chemical Physics* 115(4):1716–1733, DOI 10.1063/1.1378322
- Hellander A (2008) Efficient computation of transient solutions of the chemical master equation based on uniformization and quasi-Monte Carlo. *The Journal of Chemical Physics* 128:154,109
- Hickernell FJ (2002) Obtaining  $O(N^{-2+\epsilon})$  convergence for lattice quadrature rules. In: Fang KT, Hickernell FJ, Niederreiter H (eds) *Monte Carlo and Quasi-Monte Carlo Methods 2000*, Springer-Verlag, Berlin, pp 274–289
- Higham DJ (2008) Modeling and simulating chemical reactions. *SIAM Review* 50(2):347–368, URL <https://doi.org/10.1137/060666457>
- Joe S, Kuo FY (2008) Constructing Sobol sequences with better two-dimensional projections. *SIAM Journal on Scientific Computing* 30(5):2635–2654
- Kloeden PE, Platen E (1992) *Numerical Solutions of Stochastic Differential Equations*. Springer-Verlag, Berlin
- Koh W, Blackwell KT (2012) Improved spatial direct method with gradient-based diffusion to retain full diffusive fluctuations. *The Journal of Chemical Physics* 137(15):154,111, DOI 10.1063/1.4758459
- Lécot C, Coulibaly I (1998) A quasi-Monte Carlo scheme using nets for a linear Boltzmann equation. *SIAM Journal on Numerical Analysis* 35(1):51–70
- L’Ecuyer P (2009) Quasi-Monte Carlo methods with applications in finance. *Finance and Stochastics* 13(3):307–349
- L’Ecuyer P (2012) Random number generation. In: Gentle JE, Haerdle W, Mori Y (eds) *Handbook of Computational Statistics*, 2nd edn, Springer-Verlag, Berlin, pp 35–71
- L’Ecuyer P (2016) SSJ: Stochastic simulation in Java, <http://simul.iro.umontreal.ca/ssj/>
- L’Ecuyer P (2018) Randomized quasi-Monte Carlo: An introduction for practitioners. In: Glynn PW, Owen AB (eds) *Monte Carlo and Quasi-Monte Carlo Methods: MCQMC 2016*, Springer, Berlin, pp 29–52
- L’Ecuyer P, Buist E (2005) Simulation in Java with SSJ. In: *Proceedings of the 2005 Winter Simulation Conference*, IEEE Press, Piscataway, NJ, pp 611–620
- L’Ecuyer P, Lemieux C (2000) Variance reduction via lattice rules. *Management Science* 46(9):1214–1235
- L’Ecuyer P, Lemieux C (2002) Recent advances in randomized quasi-Monte Carlo methods. In: Dror M, L’Ecuyer P, Szidarovszky F (eds) *Modeling Uncertainty: An Examination of Stochastic Theory, Methods, and Applications*, Kluwer Academic, Boston, pp 419–474
- L’Ecuyer P, Munger D (2016) Algorithm 958: Lattice builder: A general software tool for constructing rank-1 lattice rules. *ACM Transactions on Mathematical Software* 42(2):Article 15
- L’Ecuyer P, Lécot C, Tuffin B (2006) Randomized quasi-Monte Carlo simulation of Markov chains with an ordered state space. In: Niederreiter H, Talay D (eds) *Monte Carlo and Quasi-Monte Carlo Methods 2004*, Springer-Verlag, Berlin, pp 331–342
- L’Ecuyer P, Demers V, Tuffin B (2007) Rare-events, splitting, and quasi-Monte Carlo. *ACM Transactions on Modeling and Computer Simulation* 17(2):Article 9, 45 pages
- L’Ecuyer P, Lécot C, Tuffin B (2008) A randomized quasi-Monte Carlo simulation method for Markov chains. *Operations Research* 56(4):958–975
- L’Ecuyer P, Lécot C, L’Archevêque-Gaudet A (2009) On array-RQMC for Markov chains: Mapping alternatives and convergence rates. In: L’Ecuyer P, Owen AB (eds) *Monte Carlo*

- and Quasi-Monte Carlo Methods 2008, Springer-Verlag, Berlin, pp 485–500
- L’Ecuyer P, Munger D, Lécot C, Tuffin B (2018) Sorting methods and convergence rates for Array-RQMC: Some empirical comparisons. *Mathematics and Computers in Simulation* 143:191–201
- Lemieux C, Cieslak M, Luttmer K (2004) RandQMC User’s Guide: A Package for Randomized Quasi-Monte Carlo Methods in C. Software user’s guide, available at <http://www.math.uwaterloo.ca/~clemieux/randqmc.html>
- Niederreiter H (1992) Random Number Generation and Quasi-Monte Carlo Methods, SIAM CBMS-NSF Reg. Conf. Series in Applied Mathematics, vol 63. SIAM
- Owen AB (1997) Scrambled net variance for integrals of smooth functions. *Annals of Statistics* 25(4):1541–1562
- Owen AB (2003) Variance with alternative scramblings of digital nets. *ACM Transactions on Modeling and Computer Simulation* 13(4):363–378
- Padgett JMA, Ilie S (2016) An adaptive tau-leaping method for stochastic simulations of reaction-diffusion systems. *AIP Advances* 6(3):035,217, DOI 10.1063/1.4944952
- Pollock DSG (1993) Smoothing with cubic splines. Tech. rep., University of London, Queen Mary and Westfield College, London
- Strehl R, Ilie S (2015) Hybrid stochastic simulation of reaction-diffusion systems with slow and fast dynamics. *The Journal of Chemical Physics* 143(23):234,108, DOI 10.1063/1.4937491
- Wächter C, Keller A (2008) Efficient simultaneous simulation of Markov chains. In: Keller A, Heinrich S, Niederreiter H (eds) *Monte Carlo and Quasi-Monte Carlo Methods 2006*, Springer-Verlag, Berlin, pp 669–684